Layer-Like Field Inhomogeneities in Homogeneous Semiconductors in the Range of "*N*-Shaped Negative Differential Conductivity"*

K. W. BÖER
Physics Department, University of Delaware, Newark, Delaware
(Received 22 March 1965)

Characteristic layer-like field inhomogeneities are shown to occur in homogeneous semiconductors if the decrease in conductivity is stronger than linear with increasing field. These inhomogeneities are discussed generally in a model using Poisson and transport equations, and the fact that the neutral density of electrons and/or the mobility decreases with increasing field strength. The method of characteristics is used for discussion in order to facilitate analysis of the experimental observations. Further experimental results about layer-like field inhomogeneities in CdS concerning domain width and field strengths, influence of optical excitation and quenching, and net charging of CdS crystals are given and show good agreement with the proposed theory.

1. INTRODUCTION

CHARACTERISTIC layer-like field inhomogeneities[1–3] in homogeneous semiconductors were first observed in CdS single crystals when the applied voltage was raised above a certain value. These inhomogeneities were made visible[1–4] by using the shift of the absorption edge with the electrical field (Franz-Keldysh effect[5,6]). Similar field inhomogeneities were observed also in other semiconductors, e.g., Ge, Si, and GaAs.[7–15]

The author proposed to explain layer-like field inhomogeneities in CdS by means of a decrease in conductivity with field strength because of field quenching.[16] Later Ridley showed that such a layer-like inhomogeneity must exist in the steady state for thermodynamic reasons, if the averaged field lies within an *N*-shaped "negative differential resistance[17]" range.[18] A similar explanation was given by Kiess and Stöckmann.[19]

A decrease in conductivity with increasing field strength can be explained by the following: (a) redistribution of electrons over levels in the band gap caused by field (field quenching)[16,19] or due to Joule heating[20,21], (b) redistribution of electrons over bands with different effective masses,[22–25] (c) field-dependent capture cross section of recombination centers (e.g., Au-doped germanium[26–29]) or field-dependent scattering mechanism (hot electrons),[30,31] and (d) the electron drift velocity becoming larger than the velocity of sound.[32–40] *All* of

* This work was supported in part by the U. S. Office of Naval Research Contract No. NONR (G) 4336 (00), and by the U. S. Army Research Office-Durham Contract No. DA-31-124-ARO(D).

[1] K. W. Böer, H. J. Hänsch, and U. Kümmel, Z. Physik **155**, 170 (1959).
[2] K. W. Böer, *Festkörperprobleme* (Friederich Vieweg und Sohn, Braunschweig, 1962), Vol. 1, pp. 38–71.
[3] K. W. Böer, J. Phys. Chem. Solids **22**, 123 (1962).
[4] K. W. Böer, H. J. Hänsch, and U. Kümmel, Naturwiss. **45**, 460 (1958).
[5] W. Franz, Z. Naturforsch **13a**, 484 (1958).
[6] I. V. Keldysh, Zh. Eksperim. i Teor. Fiz. **34**, 1138 (1958) [English transl.: Soviet Phys.—JETP **6**, 788 (1958)].
[7] R. G. Pratt and B. K. Ridley, Proc. Phys. Soc. **81**, 996 (1963).
[8] R. G. Pratt and B. K. Ridley, Phys. Letters **4**, 300 (1963).
[9] A. Barraud, Compt. Rend. **256**, 3632 (1963).
[10] B. K. Ridley and R. G. Pratt, in *Proceedings of the International Conference on the Physics of Semiconductors, Paris, 1964* (Academic Press Inc., New York, 1965), p. 487.
[11] V. P. Sondayevsky, V. I. Stafeyev, and E. I. Karakushan, in *Proceedings of the International Conference on the Physics of Semiconductors, Paris, 1964* (Academic Press Inc., New York, 1965), p. 481.
[12] E. H. Putley, in *Proceedings of the International Conference on the Physics of Semiconductors, Paris, 1964* (Academic Press Inc., New York, 1965), p. 443.
[13] V. I. Stafeyev, Fiz. Tverd. Tela. **5**, 3095 (1963) [English transl.: Soviet Phys.—Solid State **5**, 2267 (1964)].
[14] K. W. Böer and A. Williges, Phys. Status Solidi **1**, K72 (1961).
[15] D. C. Northrop, P. R. Thornton, and K. E. Trezise, Solid-State Electron. **7**, 17 (1964).
[16] K. W. Böer, Z. Physik **155**, 184 (1959).
[17] Better "negative differential conductivity," since a negative differential resistance may be hidden by the occurrence of layer-like field inhomogeneities. Only current saturation may be observed instead. (Stabilization of *N*-shaped negative differential resistance with external resistors is impossible as can be seen by correcting a calculation error in Ref. 18.)
[18] B. K. Ridley, Proc. Phys. Soc. **82**, 954 (1963).
[19] H. Kiess and F. Stöckmann, Phys. Status Solidi **4**, 117 (1964).
[20] K. W. Böer and U. Kümmel, Phys. Status Solidi **1**, 730 (1961).
[21] E. Nebauer and E. Jahne, Phys. Status Solidi **8**, 881 (1965).
[22] H. Krömer, Phys. Rev. **109**, 1856 (1958).
[23] A. L. Zakharov, Zh. Eksperim. i Teor. Fiz. **38**, 665 (1960) [English transl.: Soviet Phys.—JETP **11**, 478 (1960)].
[24] J. B. Gunn, Solid State Commun. **1**, 88 (1963).
[25] J. B. Gunn, *International Conference on Semiconductors, Plasma Effects in Solids, Paris, 1964* (Academic Press Inc., New York, 1965), p. 199.
[26] W. L. Bonch-Bruevich, Fiz. Tverd. Tela. **6**, 2047 (1964) [English transl.: Soviet Phys.—Solid State **6**, 1615 (1965)].
[27] B. K. Ridley and R. G. Pratt, J. Phys. Chem. Solids **26**, 21 (1965).
[28] R. G. Pratt and B. K. Ridley, J. Phys. Chem. Solids **26**, 11 (1965).
[29] V. L. Bonch-Bruevich and S. G. Kalashnikov, *International Conference on Semiconductors, Plasma Effects in Solids, Paris, 1964* (Academic Press Inc., New York, 1965), p. 193, and Fiz. Tverd. Tela **7**, 750 (1965) [English transl.: Soviet Phys.—Solid State **7**, 599 (1965)].
[30] J. B. Gunn, IBM J. Res. Develop. **8**, 141 (1964).
[31] K. W. Böer, Monatsber. Deut. Akad. Wiss. Berlin **1**, 325 (1959).
[32] V. L. Gurevich, V. D. Kagan, and B. D. Laichtman, *Proceedings of the International Conference on the Physics of Semiconductors, Paris, 1964* (Academic Press Inc., New York, 1965), p. 565.
[33] A. R. Hutson, J. H. McFee, and D. L. White, Phys. Rev. Letters **7**, 237 (1961).
[34] A. R. Hutson and D. L. White, J. Appl. Phys. **33**, 40, 2547 (1962); A. R. Hutson, Phys. Rev. Letters **9**, 296 (1962).
[35] A. R. Moore and R. W. Smith, *Proceedings of the International Conference on the Physics of Semiconductors, Paris, 1964* (Academic Press Inc., New York, 1965), p. 575; A. R. Moore, Phys. Rev. Letters **12**, 47 (1964).
[36] R. W. Smith, Phys. Rev. Letters **9**, 87 (1962).
[37] P. O. Sliva and R. Bray, Phys. Rev. Letters **14**, 372 (1965).
[38] J. H. McFee, J. Appl. Phys. **34**, 1548 (1963).
[39] H. Kröger, E. W. Prohofsky, and H. R. Carleton, Phys. Rev. Letters **12**, 555 (1964).
[40] E. W. Prohofsky, Phys. Rev. **136**, A1731 (1964).

these mechanisms may result in negative differential conductivity. In this paper, however, we will restrict ourselves to the discussion of (a) and (c) and indications as to how this method can be modified in order to include (b). Effects at low field and high current densities (Joule's heating) and (d) will be excluded.

In homogeneous crystals, layer-like field inhomogeneities were often found to move,[1,9,15,37] periodically appearing at the cathode and disappearing at the anode (n-type material), thereby causing characteristic current[1,2,16,41] or luminescence[42,43] oscillations,[44] which, in turn, are often used to indicate the presence of these field inhomogeneities.[7–14,45,46] However, in CdS it was observed that the high-field domain remains adjacent to the cathode or to a crystal imperfection when the voltage is not too high. It therefore seems that there are two distinct mechanisms involved, one for the formation of the field layer, and one for the movement[18] of this layer; only the former will be the subject of this paper. Stationary solutions of the Poisson and transport equations in a one-dimensional homogeneous crystal will be discussed for a general reaction-kinetic model.[47] Necessary and sufficient conditions for the occurrence of layer-like field inhomogeneities will be presented. Quantitative calculations of a simplified model will be given. Experimental results for CdS single crystals will be described which show good agreement with the theory.

2. THEORY

2.1. General Model

Assuming an n-type semiconductor or photoconductor, the charge densities are denoted by n (electrons in the conduction band), p (holes in the valence band),

$$n_{tr}=\int_{\mathcal{E}_F}^{\mathcal{E}_C} n_{tr}(\mathcal{E})d\mathcal{E}\ \text{(trapped electrons)},$$

and

$$p_{tr}=\int_{\mathcal{E}_V}^{\mathcal{E}_F} p_{tr}(\mathcal{E})d\mathcal{E}\ \text{(trapped holes)};$$

$n_{tr}(\mathcal{E})$ and $p_{tr}(\mathcal{E})$ are the respective densities per unit energy, $\mathcal{E}_C$ is the lower edge of the conduction band, $\mathcal{E}_V$ is the upper edge of the valence band, and $\mathcal{E}_F$ is the Fermi level. The Poisson and transport equations then read

$$\begin{aligned}\operatorname{div}\mathbf{E}&=(-e/\epsilon\epsilon_0)(n+n_{tr}-p-p_{tr})\\ \mathbf{J}&=en\mu\mathbf{E}-\mu kT\ \operatorname{grad}n.\end{aligned}\tag{1}$$

For a single relevant linear dimension in a crystal with field-independent mobility and neglible free hole density $p\ll p_{tr}$, and for steady-state conditions, Eq. (1) leads to[47,48]

$$\begin{aligned}dE/dx&=(e/\epsilon\epsilon_0)(n+n_{tr}-p_{tr}),\\ dn/dx&=(e/kT)(nE-j/e\mu),\\ dj/dx&\equiv 0.\end{aligned}\tag{2}$$

The solutions of Eq. (2) are curves in (n,E,x) space. However, since Eq. (2) does not contain x explicitly and has continuous partial derivatives with respect to E and n (Lifshitz condition), it is sufficient to discuss these solutions as their projection onto the (n,E) plane, and the field of direction is well-defined at all points except singular points (method of characteristics). As shown in Ref. 47, the introduction of two auxiliary functions, $n_1(E)$ for which $dE/dx\equiv 0$ (quasi-neutrality curve),[49] and $n_2(E)$ for which $dn/dx\equiv 0$ (drift-current curve) markedly simplifies this discussion. In Fig. 1 both curves are shown for a simplified case which, however, contains all essential elements for the desired discussion: The neutrality density of electrons $n_1(E)$ has a constant region, a decreasing region (e.g., field quenching), and

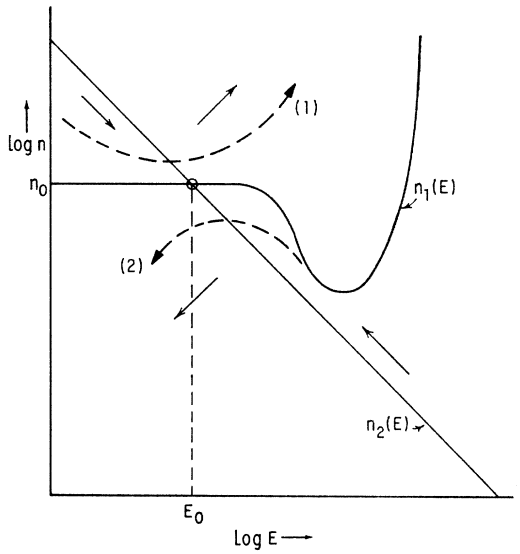

FIG. 1. Field of directions with quasi-neutrality curve $n_1(E)$ and drift current curve $n_2(E)$.

[41] J. Dziesiaty, E. Gutsche, and H. J. Rohde, Phys. Status Solidi **2**, K211 (1962).
[42] K. W. Böer and K. H. Zschauer, Phys. Status Solidi **1**, K36 (1961).
[43] C. H. Hazoni (private communication).
[44] Current oscillations in CdS and ZnSe crystals have been observed earlier without attributing these oscillations to layer-like field inhomogeneities [S. H. Liebson, J. Electrochem. Soc. **62**, 523 (1955); E. E. Loebner under Contract DA-36-039sc71194, Army Report No. 2, 1956 (unpublished); R. H. Bube and E. L. Lind, Phys. Rev. **110**, 1040 (1958)].
[45] M. Kikuchi, J. Appl. Phys. (Japan) **3**, 448 (1964).
[46] J. Okada and H. Matino, J. Appl. Phys. (Japan) **3**, 698 (1964).
[47] K. W. Böer and W. E. Wilhelm, Phys. Status Solidi **3**, 1704 (1963).
[48] K. W. Böer, *Proceedings of the International Conference on the Physics of Semiconductors, Paris, 1964* (Academic Press Inc., New York, 1965), p. 987.
[49] This procedure has the advantage that the subsequent discussion depends essentially on the qualitative behavior of the given neutrality concentration of conduction electrons and therefore is not very sensitive to changes in the reaction-kinetic model.

an increasing region (field excitation)[50] with increasing field strength. $n_1(E)$ and $n_2(E)$ divide Fig. 1 into four sectors with different sign combinations of dE/dx and dn/dx (directions of solution curves, which are represented by the four solid arrows). Since $n_1(E)$ can be crossed by solutions of Eq. (2) only along $E=$ const and $n_2(E)$ only along $n=$ const, it is obvious that there exists no solution which circles the singular point; thus in the configuration given in Fig. 1, besides the trivial solution $E=$ const, $n=$ const, there exist only solutions which cause the entire crystal to become charged, and which are indicated by the two dotted arrows. These solutions represent well-known cases of field inhomogeneities due to injecting or blocking contacts [see (1) and (2), respectively, in Fig. 1]; however, for neutral contact conditions the trivial solution is the only one allowed, leading to $E=E_0=V/L$ ($V=$ applied voltage, $L=$ distance between electrodes). As was shown earlier,[47] with increasing V the drift-current curve $n_2(E)$ shifts parallel to itself towards higher values, and a qualitative change in solution curves must occur at the latest at a position (b) given in Fig. 2. This is most easily seen by using continuity arguments to conclude that the singular point (I) is the only possible trivial solution with increasing voltage up to $V_{\text{crit}}=E_{\text{crit}}L$. An *infinitesimal* increase in applied voltage above V_{crit} causes (I) to disappear, but the singular point (III) cannot represent a physically meaningful solution at this voltage since its connected field E_3 is separated from E_{crit} by a *finite* amount. However, following the entropy discussion of Ridley[18] and Ries and Stöckmann,[19] one can see that already at voltages below V_{crit}, namely, above $V_1=E_1L$ in Fig. 2, an inhomogeneous solution may occur. This solution may start near the singular point (II,III) and run between $n_1(E)$ and $n_2(E)$ towards the singular point (I), as indicated by the arrow in Fig. 2. The condition

$$\int_0^L E(x)dx=V$$

determines how close to (II,III) the solution has to start.[51] In order to see this, it is advantageous to discuss a more simplified model.

2.2. Model Neglecting Diffusion Current

It is easy to see that, in the transport equation, the diffusion part can be neglected, since it is small compared to the drift part as soon as the voltage drop across a Debye length is of the order of one volt or higher. This is fulfilled in the experimentally observed

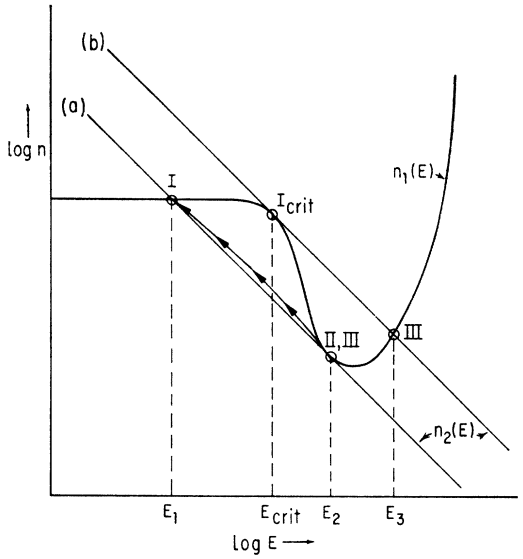

FIG. 2. Quasi-neutrality curve $n_1(E)$ and drift-current curves $n_2(E)$ for two characteristic positions (a) minimum and (b) maximum position in the range of layer-like field inhomogeneities.

case in CdS,[52] where the space-charge region is less than 0.1 mm thick; the voltage drop across this region is more than 1000 V, and for the observed[53] electron density of about 10^{10} cm^{-3} the Debye length is $(\epsilon\epsilon_0 kT/2e^2n)^{1/2}$ $\simeq 10^{-3}$ cm.

Therefore Eq. (2) reduces to

$$\begin{aligned} dE/dx&=-(e/\epsilon\epsilon_0)(n+n_{\text{tr}}-p_{\text{tr}}),\\ j&=e\mu nE,\\ dj/dx&\equiv 0, \end{aligned} \tag{3}$$

and one can plot a current axis along the bisector of the ln$n$-versus-ln$E$ plane (Fig. 3). From this diagram a current-voltage characteristic can be obtained directly, which, for the homogeneous case, is Ohmic up to $V_1=E_1L$ (see Fig. 3). With further increasing voltage the current increases if the solution remains homogeneous. However, an inhomogeneous solution of the kind described in 2.1 also exists, for which the current stays constant at j_0 up to $V_2=E_2L$, as will be shown for a simplified model in 2.3. For thermodynamic reasons the situation with lowest entropy production, i.e., with the lowest current, is favored. Therefore, as soon as V_1 is surpassed, the crystal tends to achieve the inhomogeneous field distribution.

2.3. Simplified Model

In order to obtain numerical results, it is necessary to further simplify the reaction-kinetic model in a

[50] The number and sequential order of regions of predominant field quenching or excitation are immaterial for further discussions.

[51] A very similar situation occurs if the quasi-neutrality-density of electrons is field-independent but the mobility decreases with increasing field. Then n_1 is constant but $n_2(E)$ may become nonmonotonic and can exhibit more than one intersection with n_1. Under these conditions similar inhomogeneous solutions can occur.

[52] K. W. Böer and W. E. Wilhelm, Phys. Status Solidi 4, 237 (1964).

[53] See the estimation of the field in Sec. 3.1. With a measured current of about 1 μA, a crystal cross section of about 10^{-3} cm^2, and a mobility of 300 cm^2/Vsec, it follows that $n=4\times10^9$ cm^{-3} for the high-field region and 5.5×10^{10} cm^{-3} for the low-field region.

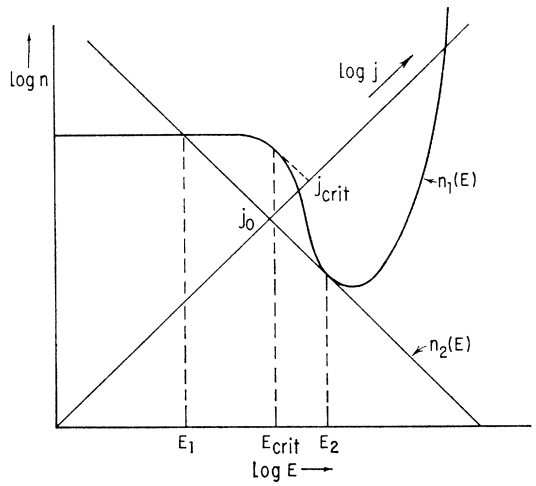

FIG. 3. Quasi-neutrality curve $n_1(E)$ and drift-current curve $n_2(E)$ with current axis j in a model neglecting diffusion current.

manner which will not, however, cause the solutions to lose their qualitative behavior, as discussed above. Such a simplified model must contain a mechanism for reducing the neutral density of electrons with increasing field. The easiest way to include such a mechanism is to introduce a field-dependent recombination process; in an essentially two-level model (Fig. 4), with

$$dn/dt = a - \gamma n p_{tr}, \tag{4}$$

(a is the number of electrons excited per cubic centimeter-second), this can be obtained by a field-dependent recombination coefficient γ which, in the simplest form, is given by a curve consisting of three linear branches. For computation, as an example, the following form of γ was used (see Fig. 5):

$$\gamma(E)=\begin{cases} 10^{-10}=\gamma_0 & \text{for } 0<E<45 \text{ kV/cm}, \\ 1.4\times10^{-12}E-6.3\times10^{-8} & \\ & \text{for } 45<E<52 \text{ kV/cm}, \\ 1.3\times10^{-14}E+9.3\times10^{-9} & \\ & \text{for } 52<E<100 \text{ kV/cm}. \end{cases} \tag{5}$$

Equation (3) simplifies to

$$\frac{dE}{dx}=-\frac{e}{\epsilon\epsilon_0}\frac{n_0}{EE_0}\left(E_0^2-\gamma_0\frac{E^2}{\gamma(E)}\right), \tag{6}$$

since $nE=n_0E_0$, where n_0 is the neutrality electron density at low fields, $n_0=(a/\gamma_0)^{1/2}$, and E_0 is given by $j=e\mu n_0E_0$. Figure 5 (lower part) gives $\gamma_0E^2/\gamma(E)$ versus E, which shows a nonmonotonic behavior and indicates that above $E_0=E(1)$ there exist more than one zeros of Eq. (6), resulting in inhomogeneous solutions for applied voltages $E(1)L<V<E(2)L$.

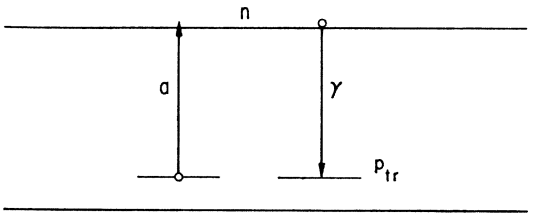

FIG. 4. Reaction-kinetic model.

At fields below $E(1)$ and above $E(2)$ only homogeneous solutions of Eq. (6) are meaningful, with $E=\text{const}=E_0$. However, in the range $E(1)<E<E(2)$ characteristic inhomogeneous solutions are found, some of which, for fields at the cathode between 47 and 54 kV/cm, are shown in Fig. 6 as obtained by numerical computation of Eq. (6). The family parameter of these curves is the applied voltage. These solution curves show a range of almost constant field near the cathode

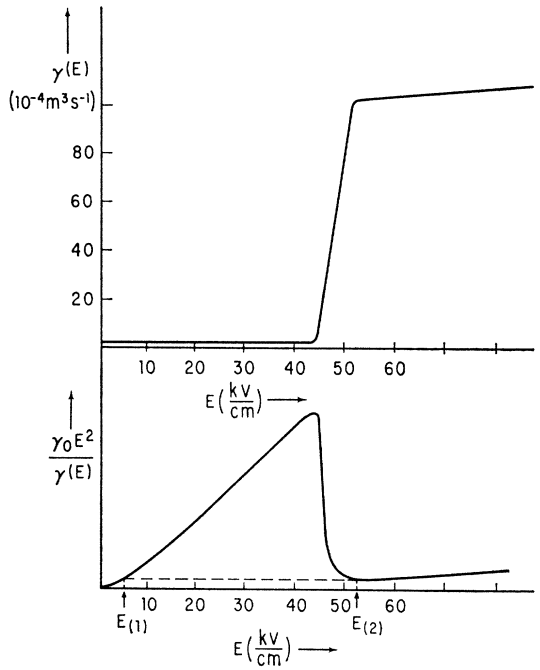

FIG. 5. Field-dependent recombination coefficient as used for the computation of [Eq. (6)], and computed $\gamma_0E^2/\gamma(E)$.

with $E\simeq E(2)$ and another near the anode with $E\simeq E(1)$. There is a relatively small transition range between these two domains; thus, in first approximation, the solution can be described as two domains only, with field strengths E_1 and E_2, the relative thicknesses of which are determined by

$$\int_0^L Edx = E_2x_1+E_1(L-x_1)=V \tag{7}$$

in agreement with the result proposed by Ridley.[18]

2.4. Discussion of the General Model

A solution of Eq. (2), indicated by the arrow in Fig. 2, similar to the one obtained above may be achieved

as soon as the applied voltage surpasses $V_1 = E_1 L$. In (n,E,x) space the solution then has the form shown in Fig. 7: It will start at the cathode close to the singular point (II,III), and remain close to E_2 up to the distance x_1 [see Eq. (7)]; then the field changes in a relatively narrow region to a value E_1 close to the singular point (I), and remains there up to the anode. This inhomogeneous solution is the only possible one for applied voltages slightly above V_{crit} according to the discussion in 2.1. In the range $V_1 < V < V_{crit}$ a homogeneous solution may be metastable (see Fig. 8).

From this, one can easily compute a current-voltage characteristic which has the form given in the lower part of Fig. 8. In the metastable range two branches are shown, for the homogeneous and the inhomogeneous case. This behavior is the same as that observed experimentally.[52]

On the other hand, from the measured current-voltage characteristic, one can directly obtain $n_1(E)$ up to E_{crit} (assuming no barrier layers) by dividing the current density j by $e\mu E_0$, and obtain the value $n_1(E_2)$ by dividing j_0 by $e\mu E_2$, which can be obtained from the domain width, as will be discussed in 3.1.

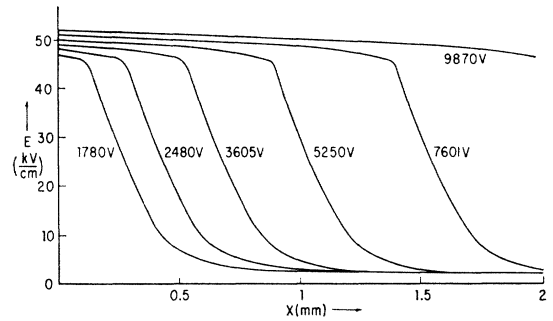

FIG. 6. Computed field in the range of layer-like field distribution from [Eq. (6)].

This theory shows that a high-field domain is produced directly adjacent to the cathode and the field decreases monotonically towards the anode, resembling a step function. The experiment often shows that this domain moves from the cathode towards the anode.[1,54–56] Since the field strengths in the high- and low-field domains remain nearly unchanged during the movement, as observed experimentally, the high-field domain must separate from the cathode according to Eq. (7), resulting in a nonmonotonic field distribution (field layer). The existence of this field maximum cannot be explained if one assumes a current drop with layer formation below its critical value in accordance to Ref. 18.

[54] K. W. Böer and U. Kümmel, Z. Angew. Phys. **12**, 241 (1960).
[55] K. W. Böer, *Proceedings of the International Conference on Semiconductor Physics, Prague, 1960* (Academic Press Inc., New York, 1961), p. 828.
[56] K. W. Böer and R. Rompe, Ann. Phys. (Germany) **7**, 3 (1960).

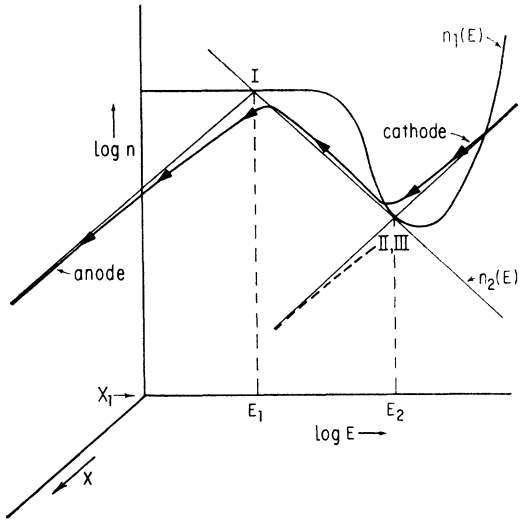

FIG. 7. Schematic solution curve $E(n,x)$ of the general model [Eq. (2)] (curve with arrows).

This can easily be seen from Fig. 2, using the experimental result that the low-field domains on the cathode and anode sides of the high-field domain have about the same field strength, which does not markedly change with domain movement. Therefore, the arrow representing the solution curve must start near (I) and end

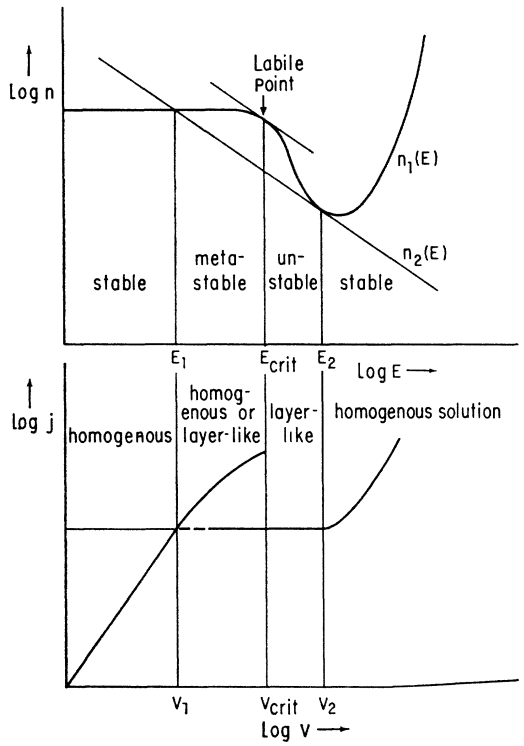

FIG. 8. Construction of the j-versus-V curve from $n_1(E)$ and $n_2(E)$: In the homogeneous case $j = e\mu n_1(E) V/L$, in the inhomogeneous case $j = \text{const} \simeq e\mu n_1(E_1) E_1 = e\mu n(E_2) E_2$.

near (I), passing the high-field layer near (II). The field of direction makes this impossible.[57]

2.5. Criterion for Field Instabilities

For field instabilities of the above-mentioned type to occur, the quasi-neutrality curve $n_1(E)$ must have a range in which its slope is negative and steeper than the slope of the drift-current curve $n_2(E)$ (see Fig. 8). Disregarding the contribution of diffusion, but allowing for a field-dependent mobility, this results in the necessary condition[31]

$$\frac{j}{e}\frac{d}{dE}\left(\frac{1}{E}\right)>\frac{d(\mu n_1)}{dE}. \tag{8}$$

If the quasi-neutrality density decreases as $n_1\sim E^{-\alpha}$ and the mobility as $\mu\sim E^{-\beta}$ in the vicinity of a maximum negative slope of $\mu(E)n_1(E)$, then Eq. (8) is fulfilled, if

$$\alpha+\beta>1, \tag{8a}$$

i.e., if the conductivity decreases faster than linearly with increasing field strength. Equation (8a) together with $V_{\text{crit}}<V<V_2$ provide the necessary and sufficient conditions under which layer-like field inhomogeneities will occur, since in this range a homogeneous field distribution cannot exist, as is shown in 2.1.

3. EXPERIMENTS AND DISCUSSION

The theory given above leads to consequences which can be checked relatively easily by experiment. In the following paragraphs a number of such experiments will be discussed. If not otherwise mentioned, the crystal dimensions were: width 1.8 mm, thickness 0.1 mm, and electrode distance 2 mm.

3.1. Influence of Applied Voltage on Domain Width

An earlier paper[52] indicates that the width of the high-field domain increases linearly with increasing applied voltage (see Fig. 13 in Ref. 52). Using the velocities of the domains, as obtained from Figs. 12(a) and 12(b) in Ref. 52,

$$s(1650\text{ V})=1.9\times10^{-3}\text{ mm/sec}$$
$$s(2260\text{ V})=2.35\times10^{-3}\text{ mm/sec},$$

and assuming a linear dependence of the velocities on applied voltage, one obtains the width d of this domain as a function of the applied voltage, as shown in Fig. 9 [curve (1)].

On another crystal the variation of the width of a high-field domain was measured directly by photometry

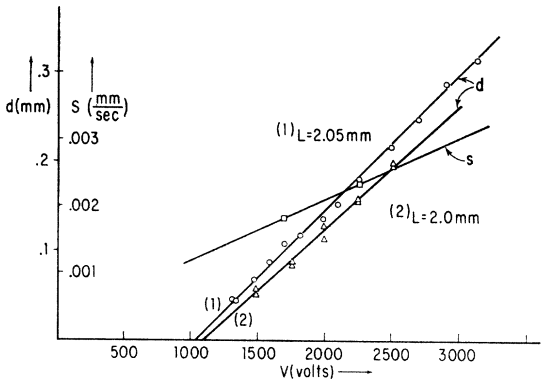

FIG. 9. Width d and velocity s of the high-field domain as a function of applied voltage L = distance between electrodes.

of absorption profiles using the Franz-Keldysh effect. In this case the domain did not separate from the cathode. Curve (2) in Fig. 9 shows d versus V for this crystal.

For both crystals the domain width is, to a good approximation, a linear function of the applied voltage, as one would expect from the simplified theory [Eq. (7)]. From these curves one can therefore determine the field strength in the low- and high-field domains:

$$E_1=\frac{V_a x_b-V_b x_a}{x_b(L-x_a)-x_a(L-x_b)}$$
and
$$E_2=\frac{V_a(L-x_b)-V_b(L-x_a)}{x_a(L-x_b)-x_b(L-x_a)} \tag{9}$$

(x_a being the position of the boundary line between the two domains for applied voltage V_a, and x_b for V_b). If the layer width is small compared with the distance L between the electrodes, the field strength of the low-field domain can, to a good approximation, be obtained from the V intercept of the d-versus-V curve

$$E_1\simeq V(d=0)/L \tag{9a}$$

and the field strength of the high-field domain from the slope of this curve

$$E_2\simeq\Delta V/\Delta d. \tag{9b}$$

From the measured curves one obtains

Crystal (1): $E_1=5.0$ kV/cm and $E_2=66$ kV/cm.
Crystal (2): $E_1=5.5$ kV/cm and $E_2=74$ kV/cm.

For the second curve the band-edge shift due to the Franz-Keldysh effect for an absorption constant $K\simeq10^2$ cm^{-1} was measured to be[58]

$$\Delta\lambda=205\pm10\text{ Å}$$

in the high-field domain, at 90°K, which agrees within

[57] However, if one forces the field at the cathode to stay low (injecting contacts) the current may rise above the critical value and an inhomogeneous solution may be achieved with rising field strength, similar to the one pointed out in an earlier paper (Ref. 47). Current oscillations of the Gunn effect seem to be caused by such forced layer production at fields corresponding to $E>E_{\text{crit}}$. (See, e.g., H. Kroemer and G. F. Day, interims Report Nos. 5 and 6 (unpublished), under Air Force Contract AF 33[657]11015, 1965).

[58] Care was taken that there was a negligible additional thermal shift of the absorption edge by choosing a photoinsensitive crystal.

10% with the value calculated by Franz:

$$\Delta\lambda=\frac{\lambda^2 he^2\beta^2}{48\pi c(kT)^2 m^*}E^2=188\text{ Å} \qquad (10)$$

using $m^*=0.2\ m_0$ and $\beta=2.4$, as obtained by Gutsche and Lange,[59] and for $E=E_2=74$ kV/cm, as calculated with Eq. (9b) from the measured curve. E_1 is in agreement with values measured with probes to within a few percent.

From the current-density-versus-applied-voltage curve and the layer width as given in Fig. 10 for crystal (2), one obtains values for the neutral-electron-density curve (see lower part of Fig. 10). The field-quenched photoconductivity of crystal (2) is lower than the unquenched value by at least a factor of $n_1(E)/n_2(E)=1/13$.

3.2. Influence of Optical Excitation

A change in the intensity of optical excitation should influence the formation of domains.[48] This can easily be seen in Fig. 11 where three contributions due to increased optical excitation are plotted schematically: (1) The increase of neutral density of electrons at low fields, shifting the horizontal part of $n_1(E)$ upwards; (2) the increase caused thereby in photoconductivity, shifting the drift-current curve $n_2(E)$ towards higher values; (3) the further separation of the quasi-Fermi levels, shifting field quenching[60] and field excitation towards lower field strengths. From this one can conclude that the critical voltage as well as E_1 and E_2 should decrease with increasing light excitation, i.e., the initiation of layer-like field inhomogeneities should occur at lower voltages; and that the horizontal part of the current-voltage characteristic should shift to lower currents.

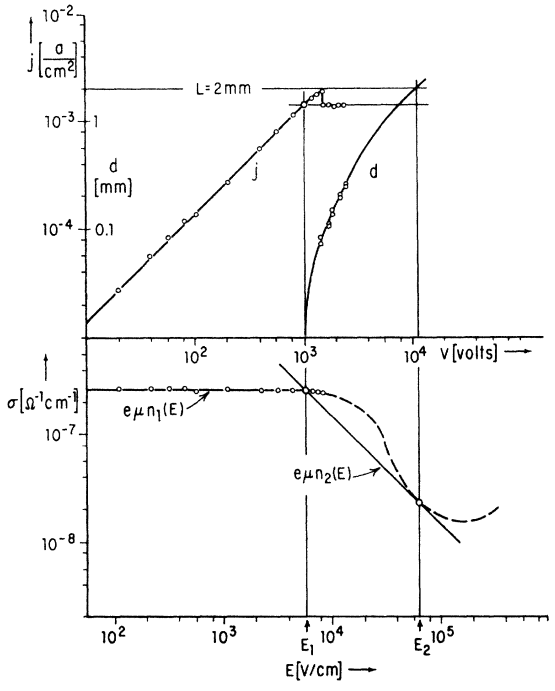

FIG. 10. Current density and layerwidth versus applied voltage and $n_1(E)$ curve for crystal (2).

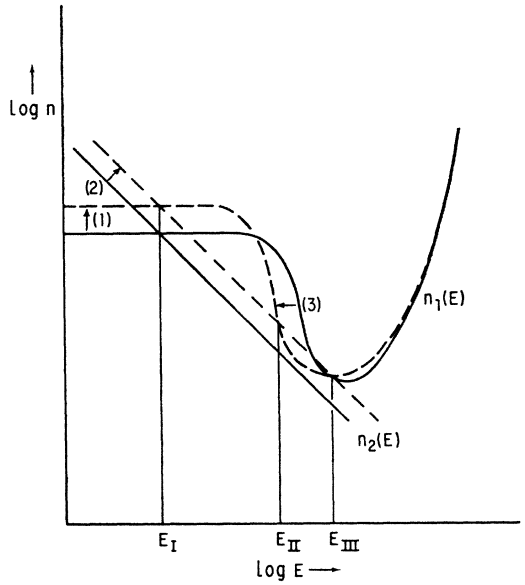

FIG. 11. Quasineutrality curves $n_1(E)$ and drift-current curves $n_2(E)$ at a certain light excitation level (solid lines) and at an increased light excitation level (dashed curves) (Schemahe).

Assuming a linear increase of photoconductivity with light excitation, $n\propto a$, the quasi-Fermi level for electrons shifts as $\mathcal{E}_{Fn}=\mathcal{E}_C+kT\ln a/a_0$, where a_0 is a proportionality constant of the dimensions of a. For field excitation from the Fermi level the excitation probability is

$$W\sim E\exp\frac{(\mathcal{E}_C-\mathcal{E}_{Fn})^{3/2}}{E}, \qquad (11)$$

and the field strength at which a given fraction of electrons is excited, i.e., at which $W=$ const, is determined by $E^{2/3}\sim\ln(a_0/a)$. Assuming the same behavior for field quenching, the field at which $n_1(E)$ decreases markedly will be shifted towards lower field strength in a similar manner. $n_2(E)$ and the horizontal part of $n_1(E)$ will be shifted towards higher values proportionally to a. This results in a reduction of V_{crit}, which can be obtained by simple geometric analysis of Fig. 11:

$$V_{\text{crit}}{}^{2/3}\propto\ln(a_0/a). \qquad (12)$$

[59] E. Gutsche and H. Lange, *Proceedings of the International Conference on the Physics of Semiconductors, Paris, 1964* (Academic Press Inc., New York, 1965), p. 129.

[60] For field quenching holes are excited by the field from hole traps into the valence band, from which they can recombine at recombination centers with conduction electrons and thereby enhance the recombination of those electrons. This effect can therefore be described by an effective field-dependent recombination coefficient as given in 2.3.

Assuming that the field-quenched neutral density of electrons [minimum of $n_1(E)$] is independent of the optical excitation, with increasing light intensity the field strengths E_1 and E_2 should be reduced in the same manner and therefore the horizontal part of the current-voltage characteristic (see Fig. 10) should also be reduced by

$$j_0^{2/3} \propto \ln(a_0/a). \tag{12a}$$

Experimental investigations show that the voltage for initiation of a layer-like field inhomogeneity decreases with increasing optical excitation. Since the range of intensities in which these inhomogeneities occur is relatively small,[61] a more precise measurement is necessary to verify Eq. (12). However, since a time lag in the metastable range precludes an exact measurement of V_{crit}, current-voltage characteristics have been measured with voltage increasing linearly with time, and the voltage V_4 at which a marked current drop is observed is used in Eq. (12) instead of the critical voltage for initiation of layer-like field inhomogeneities (assuming $V_4 \sim V_{\text{crit}}$). Figure 12 shows results of measurements on a crystal within the range in which the photoconductivity varies linearly with light intensity, and shows good agreement with Eq. (12).

However, the horizontal part of the characteristic j_0 increases with increasing optical excitation, in disagreement with Eq. (12a). This indicates that the assumption used for Eq. (12a), that the minimum value of $n_1(E)$ is independent of the optical excitation, is not fulfilled. The field quenching obviously becomes less effective with increasing excitation, as is often found for optical quenching. This effect should limit the effectiveness of increased excitation in enhancing the formation of layer-like field inhomogeneities; therefore, only in a range of medium intensity does optical excitation seem to be favorable for these inhomogeneities. Thermal effects (Joule heating) at higher intensities prevented further experimental investigations of the undisturbed field-quenched case.

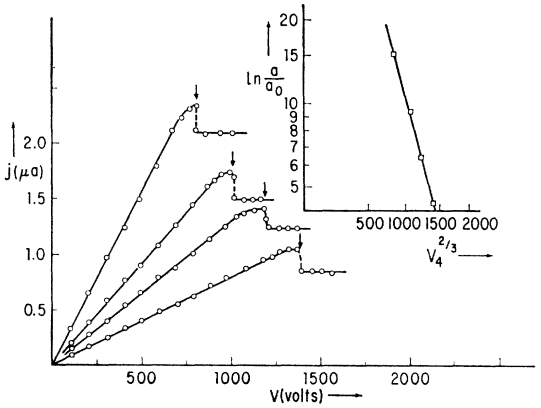

FIG. 12. Current-voltage characteristic for four different light intensities with initiation of layer-like field inhomogeneities (arrows) and the dependence of the initiation voltage V_4 on the light intensity a for crystal (4).

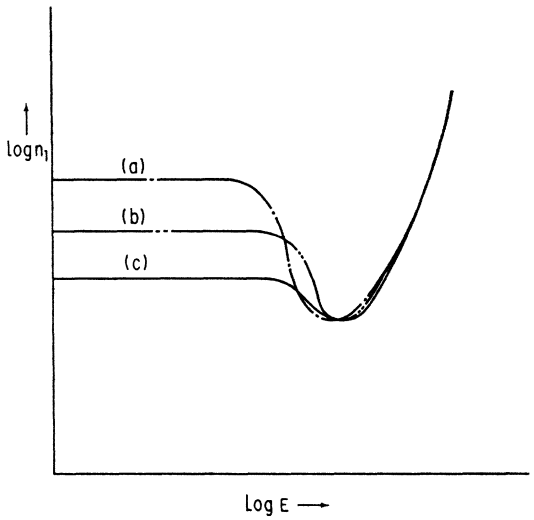

FIG. 13. Quasi-neutrality curves for increased additional IR irradiation [from (a) to (c)] (schematic).

3.3. Influence of Infrared Quenching

Optical quenching acts as a competing effect against field quenching which, in CdS at high fields and low current densities, is the essential effect causing layer-like field inhomogeneities.[62] With increasing infrared quenching the horizontal part of the neutral density curve $n_1(E)$ decreases and the field quenching becomes less and less pronounced (see Fig. 13), i.e. the slope of the decreasing part of $n_1(E)$ becomes shallower with increasing E. It is to be expected that above a certain infrared (IR) intensity the slope decreases below the critical slope given in Eq. (8a); thus layer-like inhomogeneities must disappear.

In the range of layer-like field inhomogeneities the current j_0 should increase with increased homogeneous IR irradiation, as can be seen from Fig. 14. Assuming the IR quenching is negligible compared to the field quenching in its maximum range, which should be the case for not too high IR intensities, the change in j_0 with IR can be estimated similarly to the discussion in Sec. 3.2: The shift of the decreasing part of $n_1(E)$ due to IR is determined by the shift of the quasi-Fermi level for holes which, in a linearized model, is given by $\mathcal{E}_{Fp} = \mathcal{E}_V + kT \ln(a_I/a_0)$ (a_I = intensity of IR light).

[61] At very low intensities the applied voltage has to be too high and usually a dielectric breakdown occurs with a discharge along one surface; at very high intensities Joule heating, and finally a thermal breakdown, occur before the critical field is reached.

[62] At high current densities layer-like field inhomogeneities can be produced by Joule heating if the crystal temperature lies within a range of negative temperature coefficient of photoconductivity (Ref. 20), or possibly also by strong electron-phonon interaction in the range in which the drift velocity exceeds the sound velocity.

From Fig. 14, and the field-quenching probability analogous to Eq. (11), one then predicts a current shift of

$$j_0^{2/3} \propto \ln(a_I/a_0); \tag{13}$$

an increase in the field strengths E_1 and E_2 is given by

$$E_{1,2}^{2/3} \propto \ln(a_I/a_0), \tag{13a}$$

resulting in a decrease in layer width at constant applied voltage of

$$\Delta x_1 = -x_1 \Delta E_2/E_2, \tag{13b}$$

where ΔE_2 is the change in E_2 due to IR.

An inhomogeneous, strong IR irradiation covering a layer parallel to the layer-like field inhomogeneity should also result in a decrease of the high-field domain width. This can easily be seen from Eq. (7), here leading to $E_2\bar{x}_1+E_1(x_2-\bar{x}_1)+E_{IR}(1-x_2)=V$, which describes the field distribution with an IR-irradiated layer between L and x_2, with a resulting field E_{IR} in this layer. The decrease in width of the high-field domain is then given by

$$\Delta x_1 = x_1-\bar{x}_1 = [(E_{IR}-E_1)/(E_2-E_1)](L-x_2). \tag{13c}$$

However, if the high-field domain is not completely quenched, the current through the crystal will not change when a layer within the crystal parallel to the domain is irradiated with quenching light. This should be true independently of whether the IR-quenched layer lies within a high- or a low-field domain, provided only that one can disregard effects at the electrodes and the influence of diffusion current.

Experimental investigations show that the width of the high-field domain decreases with increasing homogeneous IR irradiation and the current through the crystal increases (Fig. 15). For low IR intensities there is satisfactory agreement with the theory [Eqs. (13)].

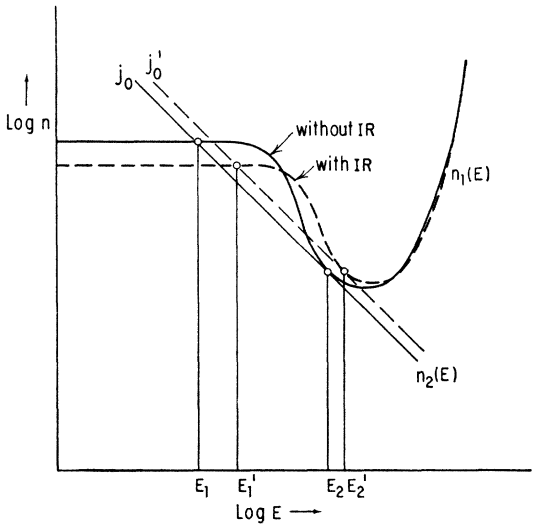

FIG. 14. Influence of IR irradiation on the given neutrality curve and the drift-current curve (schematic).

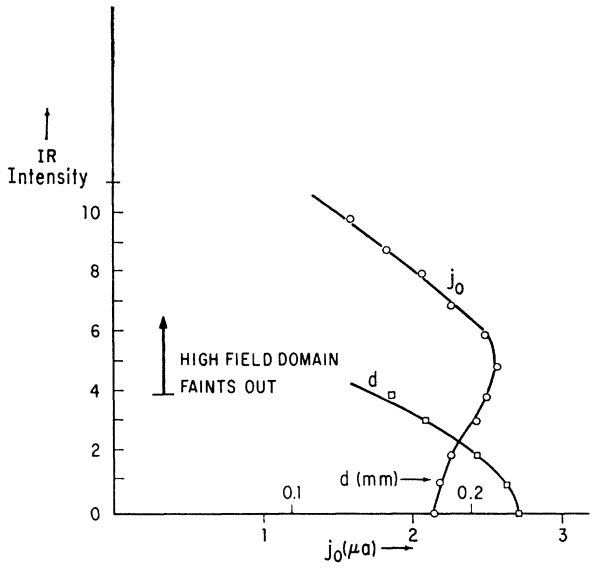

FIG. 15. Change of current j and domain thickness d with increased homogeneous IR irradiation at $\lambda=950$ mμ [crystal (3)].

With further increasing IR, the high-field domain disappears, and from here on the current through the crystal decreases (Fig. 15).

The IR intensity at which the layer-like field inhomogeneity is completely quenched increases with increasing applied voltage according to Eq. (13a), as has been observed and reported earlier.[48]

A layer-like IR irradiation can quench part of the high-field domain, as theoretically predicted above and shown in a series of photographs[63] in Fig. 16. If care was taken that the IR layer was focused onto an inner part of the crystal only, preventing stray light from hitting the remainder of the crystal and especially the boundaries of the electrodes, the current was observed to stay constant within $\pm 8\%$ until, with increased width and intensity of the IR irradiation, the entire high-field domain was quenched. Then the current decreases in a manner similar to that shown in Fig. 15.

3.4. Electrostatic Charging of the Crystal

The net electrostatic charge of a crystal is a measure of the difference of field strengths at the cathode and anode,

$$\int_c^a \rho(x)dx = E_a - E_c. \tag{14}$$

It can easily be measured by dropping the crystal out of a pair of contact tweezers into the beaker of an electrometer after it has been exposed to an applied

[63] J. Green, Master thesis, Univ. of Delaware, Tech. Rept. U. S. Army Res. Office Durham, DA-31-124 ARO(D)-173, 1964 (unpublished).

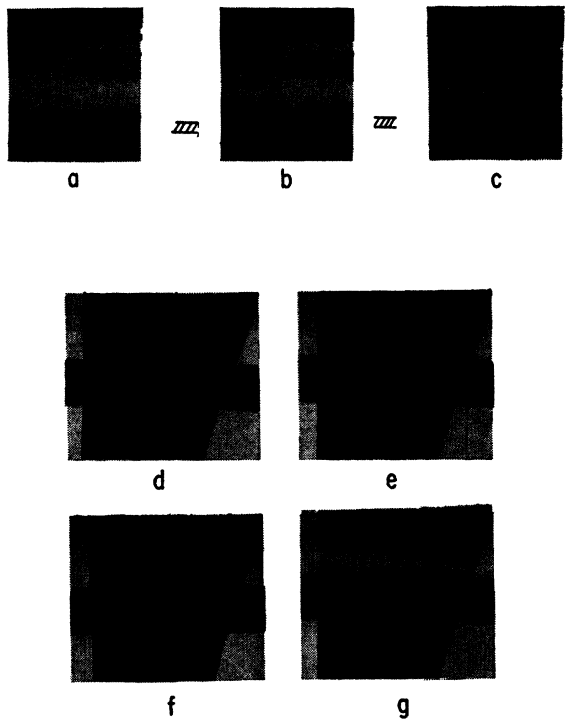

FIG. 16. Photographs of CdS crystals in monochromatic light at the absorption edge ($\lambda = 498$ mμ) at -110°C, in order to make field distributions visible using the Franz-Keldysh effect. The dark areas at the top and bottom of all photographs are the electrodes, the lines at the upper part of (a)–(c) are crystal striations, and the black bar in the middle of (d)–(g) is a shadow, used for artificial initiation of layer-like field inhomogeneities. (a) shows a layer-like field inhomogeneity at the lower electrode (slightly disturbed by crystal inhomogeneities); (b), same as (a) but with band of 900-mμ irradiation at position indicated at the edge of the photograph, showing quenching of the layer predominantly in this band; (c), same as (a) but with homogeneous additional 900-mμ irradiation, shows almost complete quenching of the layer; (d) without field; (e) with field, showing layer above shadow; (f) with band of 900-mμ irradiation in position indicated by 700-mμ irradiation in (g). Applied voltage 2500 V. Crystals (5) and (6); electrode distance 1.5 mm; crystal current range 1–5 μA.

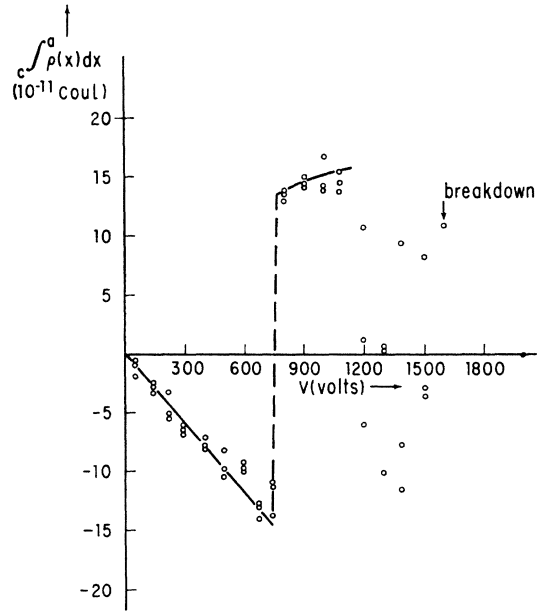

FIG. 17. Net charge of CdS platelet as a function of the applied voltage before dropping the crystal into the beaker of an electrometer. Crystal (7); electrode distance 0.19 mm; maximum current before breakdown 2×10^{-6} A.

voltage.[64,65] It is known that with indium contacts and no illumination the crystal always becomes negatively charged,[64] indicating injecting contacts and lower fields at the cathode than at the anode. However, with light excitation (extrinsic excitation carefully applied to ensure as homogeneous an illumination as possible) there is an abrupt change of sign in the net charge, if the applied voltage surpasses a critical value (Fig. 17), indicating that now the highest field is located at the cathode.[66] This critical voltage is found to be identical to the one at which a slight decrease in current shows the initiation of a layer-like field inhomogeneity. At still higher voltages drastic fluctuations of the net charge have been observed, indicating a separation of the layer from the cathode and its movement through the crystal which also shows up in current oscillations.

4. CONCLUSION

The occurrence of layer-like field distributions in the prebreakdown range as, e.g., in CdS, they can be observed visually by electro-optical methods, can be understood with a simple, one-dimensional model using Poisson and transport equations with drift and diffusion terms[67] for one type of carrier only and a mechanism which causes the conductivity to decrease more rapidly than linearly with increasing field.

The theoretical discussion of time-independent solutions uses the method of characteristics with quasi-neutrality- and drift-current curves, which proves to be very useful for a simple analysis of the experimental behavior.

The field distribution obtained from the theory is homogeneous at applied voltages below a certain V_1, and necessarily inhomogeneous at voltages between V_{crit} and V_2. For voltages between V_1 and V_{crit} a homogeneous solution can be metastable, apart from the stationary inhomogeneous solution.

The essential features of the inhomogeneous solution can be described as a high-field domain at the cathode and a low-field domain at the anode, with roughly constant fields in these domains, and a relatively small transition region resulting in a decreased current compared to the homogeneous solution. A separation of the

[64] K. W. Böer, U. Kümmel, and K. E. Schroeter, Z. Physik **167**, 403 (1962).
[65] W. Ruppel, Helv. Phys. Acta. **31**, 311 (1958).
[66] The electrodes were pressed-on indium contacts and seem to be not perfectly injecting.
[67] The diffusion is not essential for this explanation.

high-field domain from the cathode is possible only between V_{crit} and V_2 and with currents above j_{crit}.

It has been observed that the applied voltage influences the domain width linearly, but does not influence the field strength in the domains. An increased optical excitation results in a reduction of the critical voltage. An increased additional IR quenching results in a decrease in the width of the high-field domain and an increase in critical voltage or, finally, at constant applied voltage, in a forced return to the homogeneous solution. Partial quenching of a layer parallel to the high-field domain results in a decrease in its width. A change in the sign of the net charge of the crystal with injecting contacts occurs as layer-like field inhomogeneities are initiated and as long as they remain adjacent to the cathode. All these experimental results are in good agreement with the proposed theory.

ACKNOWLEDGMENTS

The author wishes to express his thanks to J. R. Green for taking the photographs in Fig. 16, to C. Ronald Simkins and Philip L. Quinn for their assistance in the computation of Eq. (6), to Professor D. E. Lamb for the use of the analog computer EAI 231-R, to M. Weaver and E. E. Ridley for the shop work, and to Philip L. Quinn, P. Massicot, and J. R. Green for helpful discussions. Particularly valuable were the numerous remarks of Professor E. H. Kerner and Professor J. H. Miller, to whom the author is especially grateful.

PHYSICAL REVIEW VOLUME 139, NUMBER 6A 13 SEPTEMBER 1965

"Zeeman" and "Dipolar" Spin Temperatures during a Strong rf Irradiation*

J. JEENER, R. DU BOIS, AND P. BROEKAERT†
Université Libre de Bruxelles, Bruxelles, Belgium
(Received 12 April 1965)

Experiments have been performed on a single crystal of CaF_2 in a large constant magnetic field (7 kG), irradiated at the exact NMR frequency of F^{19} with transverse rf magnetic fields much larger than the local field. The results demonstrate the existence, in the steady state under very strong irradiation, of two independent quasi-invariants of the motion and of two corresponding temperatures which are the rotating-frame analogs of the usual laboratory-frame Zeeman and dipolar energies and temperatures in the absence of irradiation. Using pulse techniques, Zeeman and dipolar order have been transferred reversibly back and forth between the laboratory frame (without rf field) and the rotating frame (with the large rf field on). No loss of order or mixing between Zeeman and dipolar order has been observed for irradiation times up to 13 msec with a rotating component of the rf field of 25 G (the local field in CaF_2 amounts to a few gauss). The rotating-frame analog of the Strombotne-Hahn oscillations has also been observed.

IT has been shown by Redfield[1] that the properties of the spin system in a solid, in the presence of a large constant magnetic field $\mathbf{H}_0$ and of a transverse rf magnetic field $\mathbf{H}_1$, can be discussed in a frame of coordinates (X,Y,Z) rotating around $\mathbf{H}_0$ at the same angular velocity as $\mathbf{H}_1$, by means of an effective Hamiltonian H_{eff} which has the same structure as the Hamiltonian H in the laboratory frame (x, y, z with z and Z in the direction of $\mathbf{H}_0$) in the absence of rf irradiation.[2] Thus one anticipates very striking similarities between the behavior of spin systems in the presence or absence of rf irradiation, and many such similarities have been observed already. For instance, saturation by irradiation at the NMR frequency ($-\gamma\hbar\mathbf{H}_0$ or $-\gamma\hbar\mathbf{H}_{eff}$)[3] and free precession signals[4] have been observed in both cases.

When the Zeeman term of the Hamiltonian is not much larger than the spin-spin coupling term ($|\mathbf{H}_0|$ or $|\mathbf{H}_{eff}| \lesssim$ a few times the local field $|H_L|$), energy is exchanged rapidly between these two terms and one expects to reach a steady-state situation characterized by a single spin temperature. This conjecture has been very successful in the interpretation of adiabatic magnetization and demagnetization experiments in both reference frames.[5]

However, when the Zeeman terms of the Hamiltonian are much larger than the spin-spin coupling term, spontaneous energy flow between these terms becomes extremely slow, and a number of recent experiments have demonstrated that the dipolar energy in the laboratory frame is a quasi-invariant of the motion in

* This research has been partially supported by the Fonds National de la Recherche Scientifique and by the Fonds de la Recherche Scientifique Fondamentale Collective.

† Predoctoral Fellow of the Institut pour l'Encouragement de la Recherche Scientifique dans l'Industrie et l'Agriculture

[1] A. G. Redfield, Phys. Rev. **98**, 1787 (1955).

[2] The fixed frame quantities $\mathbf{H}_0$ and H_D (spin-spin coupling Hamiltonian) are replaced in the rotating frame by $\mathbf{H}_{eff}$ (of the order of $\mathbf{H}_1$) and $H_D{}^0$ (that part of H_D which commutes with the fixed frame Zeeman Hamiltonian). Spin lattice relaxation will be ignored in the present discussion.

[3] See for instance A. Abragam *The Principles of Nuclear Magnetism* (Clarendon Press, Oxford, England, 1961).

[4] W. I. Goldburg and M. Lee, Phys. Rev. Letters **11**, 255 (1963).

[5] C. P. Slichter and W. C. Holton, Phys. Rev. **122**, 1701 (1961).

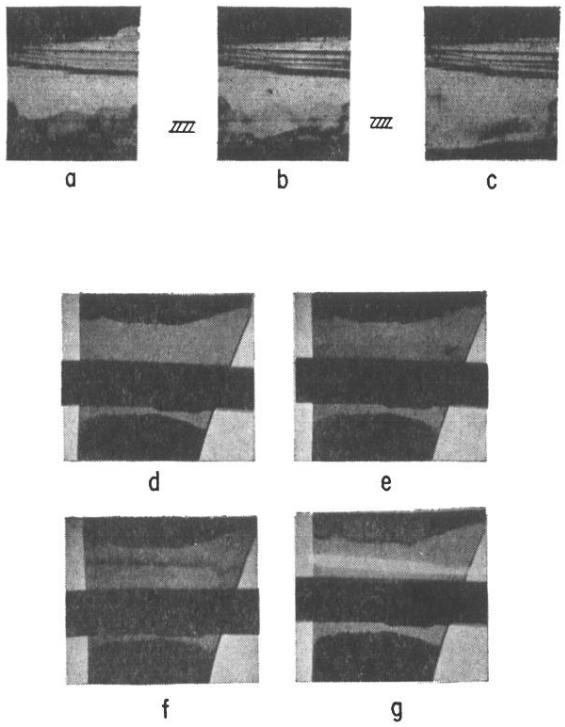

FIG. 16. Photographs of CdS crystals in monochromatic light at the absorption edge ($\lambda = 498$ mμ) at -110°C, in order to make field distributions visible using the Franz-Keldysh effect. The dark areas at the top and bottom of all photographs are the electrodes, the lines at the upper part of (a)–(c) are crystal striations, and the black bar in the middle of (d)–(g) is a shadow, used for artificial initiation of layer-like field inhomogeneities. (a) shows a layer-like field inhomogeneity at the lower electrode (slightly disturbed by crystal inhomogeneities); (b), same as (a) but with band of 900-mμ irradiation at position indicated at the edge of the photograph, showing quenching of the layer predominantly in this band; (c), same as (a) but with homogeneous additional 900-mμ irradiation, shows almost complete quenching of the layer; (d) without field; (e) with field, showing layer above shadow; (f) with band of 900-mμ irradiation in position indicated by 700-mμ irradiation in (g). Applied voltage 2500 V. Crystals (5) and (6); electrode distance 1.5 mm; crystal current range 1–5 μA.